Modeling Cardiac Stimulation by a Pacemaker, with Accurate Tissue-Electrode Interface

Valentin Pannetier, Michael Leguèbe, Yves Coudière, Richard D Walton, Philippe Dhiver, Delphine Feuerstein, Diego Amaro

Modeling Cardiac Stimulation by a Pacemaker, with Accurate Tissue-Electrode Interface

Valentin Pannetier[1], Michael Leguèbe[1,2], Yves Coudière[1(✉)], Richard Walton[3], Philippe Dhiver[4], Delphine Feuerstein[4], and Diego Amaro[4]

[1] Univ. Bordeaux, CNRS, Inria, Bordeaux INP, IMB, UMR 5251, IHU Liryc, 33400 Talence, France
valentin.pannetier@math.u-bordeaux.fr
[2] Inria, 33400 Talence, France
[3] Univ. Bordeaux, Inserm, CRCTB, U 1045, IHU Liryc, 33000 Bordeaux, France
[4] Microport CRM, Clamart, France

Abstract. In this paper we model a cardiac pacemaker placed in a bath with a cardiac excitable tissue. We take into account electrochemical phenomena observed at the electrodes during pacing by using equivalent circuits, whose parameters are calibrated with respect to bench tests data. The complete model consists of a pacemaker model coupled to a re-scaled cardiac ionic model through these circuits. It is compared with ex-vivo experimental data of stimulation threshold detection. We perform an additional study of the influence of the scaling parameters, that can help matching experimental results.

1 Introduction

An implantable pacemaker aims to restore a cardiac beat when the intrinsic conduction system fails. It sends energy to the heart in the form of a voltage pulse for a certain duration via pacing leads implanted inside the heart. The device is programmed to deliver enough energy to trigger a cardiac depolarization (which is called *capture*). For battery saving reason, the energy must be just above the cut-off threshold between capturing and non-capturing regions of the voltage – duration plane, known as the Lapicque curve [2]. We aim to reproduce by computer modeling and simulation the experimental tests run to identify this curve. This would ultimately enable manufacturers to try out and optimize the delivered energy of several leads with different electrode shapes in-silico, instead of prototyping, manufacturing and testing leads experimentally.

We propose to couple a computational model of cardiac excitable cells (tissue) in an electrolyte (blood) to a model of the pacemaker's circuitry, through interfaces located at the metal electrodes of the leads. Modeling these interfaces by themselves is an extensive field of research, because many complex biophysical phenomena occur when an electrode delivers current into an electrolyte, as compiled in [3], and because a large part of the energy is dissipated by the contacts. It is then crucial to model correctly these bio-electrode interfaces, in order to

O. Bernard et al. (Eds.): FIMH 2023, LNCS 13958, pp. 194–203, 2023.
https://doi.org/10.1007/978-3-031-35302-4_20

reproduce quantitatively the threshold voltages. Cardiac simulations generally consider only the myocardium, and apply an artificial, irrealistic stimulation. Instead, we introduce boundary conditions that include impedance of the contacts, and act as current source of the cardiac model, following the approach of Somersalo *et al.* [4].

In this paper, Sects. 2, 3, and 4, describe the complete modeling approach, model calibration with respect to experimental data, and comparison of computed Lapicque curves to experimental ones.

2 Pacemaker Model Coupled to Cardiac Ionic Equations

Pacemaker Circuit. We model the electronics of the pacemaker with the circuit shown in Fig. 1 (left), which appeared to be standard among manufacturers. We focus on the short time interval dedicated to pacing, ignoring the sensing ability of the device, as it is not linked directly to the triggering of a cardiac action potential. A tank capacitor C_{pulse} (~ 10 μF) is charged (not modelled here), and then the actual pacing follows the three steps below (see Fig. 2).

Pulse. When the device triggers a stimulation, the tank capacitor acts as source of current. In the meantime, a secondary capacitance C_{ocd} is charged. The duration of this step is programmed by the clinician, and can range from 0.25 to 2 ms. The amplitude of the stimulation, proportional to the charge of the tank capacitor, is also programmable, typically between 0.25 V and 2 V.

Switch. There is a short transition phase (in the order of hundreds of μs) during which the two switches are open (see Fig. 1, left, black part).

Output Capacitor Discharge (OCD). The capacitor C_{pulse} is isolated from the circuit, and C_{ocd} discharges. This step lasts for 13 ms and is intended to discharge the equivalent capacity due to the polarization of the electrodes that occurs during the pulse (see below).

After the OCD, the stimulating part of the device is switched off, and is replaced by a sensing circuit until the next stimulation. In the meantime, the tank capacitor C_{pulse} is recharged. During the pulse and OCD steps, the circuit can be simplified into an equivalent RC series circuit. In the following, we simply denote by R and C the equivalent resistance and capacitance of this simplified circuit, specifically, $\frac{1}{C} = \frac{1}{C_{\text{pulse}}} + \frac{1}{C_{\text{ocd}}}$ during the pulse and $\frac{1}{C} = \frac{1}{C_{\text{ocd}}}$ during OCD, while $R = R_{\text{pulse}} + R_{\text{gnd}}$ during the pulse and $R = R_{\text{gnd}}$ during OCD.

Modeling the Bio-Electrode Contacts. Multiple electrochemical interactions occur in the vicinity of the surface of an electrode placed in an electrolyte when a current is applied, as described extensively in [3]. These interactions are modeled by equivalent electric circuits, called contact models. There exists a large collection of contact models, as reviewed in [3]. We choose to model the tip and ring contacts by a resistance in parallel with a capacitance (parallel R-C, see Fig. 1, green part). This model is a good compromise that can reproduce experimental measures while relying on a limited number of parameters that

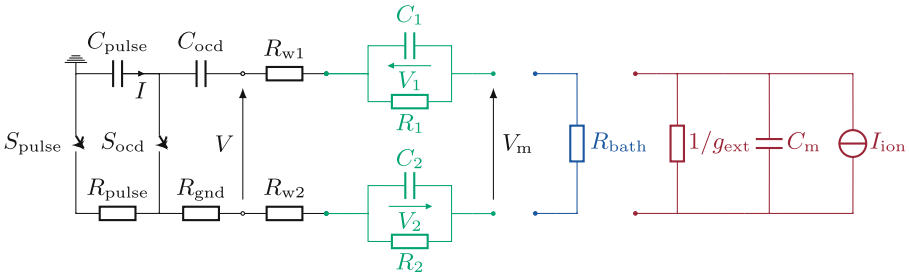

Fig. 1. Equivalent circuit of a pacemaker (black, left) coupled to either a resistive medium (blue, middle), or a single cell model (red, right) via connecting dots. On the left circuit, S_{pulse} is closed and S_{ocd} is open during the pulse step, S_{pulse} and S_{ocd} are open during switch step, S_{pulse} is open and S_{ocd} is closed during the OCD step. The resistances R_{pulse} and R_{gnd} are located within the canister of the pacemaker, whereas the resistances R_{w1} and R_{w2} are equivalent resistances for the wires between the canister and the leads.

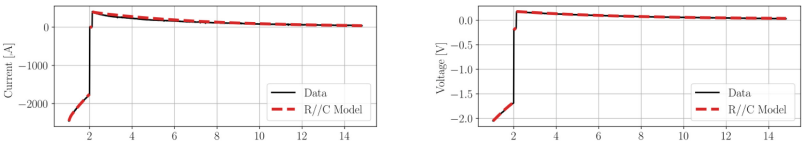

Fig. 2. Current (left) and voltage (right) delivered by a pacemaker lead in a saline solution (black solid line), between the tip and ring electrodes. Red dashed lines are the result of the calibration (Sect. 3). The voltage and duration set on the device were 2 V and 1 ms. (Color figure online)

can, in consequence, be identified. For instance, a simple resistive-only model of contact cannot reproduce the charging behavior of the bio-electrode contact, either during the pacing step nor during the switch step. On the other hand, the parameters of a complex Cole-Cole model cannot be identified from our data.

We state the equations of the contacts and pacemaker model, during pulse and OCD, as follows:

$$\frac{\mathrm{d}I}{\mathrm{d}t} + \frac{1}{\tau} I = \frac{1}{R_{\text{tot}}} \left(\frac{V_1}{\tau_1} + \frac{V_2}{\tau_2} \right), \tag{1a}$$

$$\frac{\mathrm{d}V_i}{\mathrm{d}t} + \frac{V_i}{\tau_i} = \frac{I}{C_i}, \quad i = 1, 2 \tag{1b}$$

where the current I, and voltages V_2 and V_1 are such as represented on Fig. 1. The other constants are $\tau_1 = R_1 C_1$, $\tau_2 = R_2 C_2$, $\tau = R_{\text{tot}} C_{\text{tot}}$, with $R_{\text{tot}} = R + R_{\text{w1}} + R_{\text{w2}} + R_{\text{bath}}$ and $\frac{1}{C_{\text{tot}}} = \frac{1}{C} + \frac{1}{C_1} + \frac{1}{C_2}$. Experimentally, the voltage

$V = V_1 + V_2 + (R_{\text{bath}} + R_{\text{w1}} + R_{\text{w2}})I$ is measured, where R_{bath} is the equivalent resistances of the saline solution.

In absence of applied current, the two contacts naturally discharge. Hence, we assume that $V_1(t = 0) = V_2(t = 0) = 0$. Meanwhile, the main capacitor is charged to its nominal capacity, corresponding to a voltage V_{stim}. In consequence, a current $I(t = 0) = -V_{\text{stim}}/R_{\text{tot}}$ initially flows out of it. This voltage V_{stim} is referred to as *the amplitude of stimulation.*

Pacemaker and Cardiac Tissue – Surrogate Model. To account for the excitability of the cardiac tissue, the resistance R_{bath} is not sufficient. It is replaced by a cardiac cell ionic model. The ionic model is adapted to account for the propagation of the electric current in the extracellular medium, of equivalent conductance g_{e}. The membrane is modeled by a capacitance C_{m} in parallel with the total ionic current I_{ion}. The intracellular path of conduction through gap junctions between cells is not taken into account in this simplification. We use the Beeler-Reuter ionic model [1], and we denote the transmembrane voltage by V_m.

As the Beeler-Reuter model is written in units per cm^2 of cell membrane, we introduce a scaling parameter S, representing a given surface of cell membrane. We assume that the total current I spreads uniformly on this surface. We also introduce the total conductance g_{e} of the extracardiac medium between the electrodes. Assuming that a volume of 1 mm^3 is relevant to this approximation, we obtain orders of magnitude of 100 cm^2 for S and 10^{-2} mS for g_{e}. However, the excited medium consists of blood and cardiac tissue, which is highly heterogeneous. Therefore, these estimates can only be seen as a starting point for any calibration procedure, and the current model as a surrogate to a complete 3D bidomain model. The coupled 0D model reads as follow

$$\frac{\mathrm{d}I}{\mathrm{d}t} + \frac{1}{\tau} I = \frac{1}{R_{\text{tot}}} \left(\frac{V_1}{\tau_1} + \frac{V_2}{\tau_2} + \frac{I_{\text{ion}}(h, V_{\text{m}})}{C_{\text{m}}} + \frac{V_{\text{m}}}{\tau_{\text{m}}} \right), \tag{2a}$$

$$\frac{\mathrm{d}V_i}{\mathrm{d}t} + \frac{V_i}{\tau_i} = \frac{I}{C_i}, \quad i = 1, 2 \tag{2b}$$

$$\frac{\mathrm{d}V_{\text{m}}}{\mathrm{d}t} + \frac{I_{\text{ion}}(h, V_{\text{m}})}{C_{\text{m}}} + \frac{V_{\text{m}}}{\tau_{\text{m}}} = \frac{I}{SC_{\text{m}}}, \tag{2c}$$

$$\frac{\mathrm{d}h}{\mathrm{d}t} + g(h, V_{\text{m}}) = 0, \tag{2d}$$

with τ, τ_1, τ_2 as above, but with $R_{\text{tot}} = R + R_{\text{w1}} + R_{\text{w2}}$ and $\frac{1}{C_{\text{tot}}} = \frac{1}{C} + \frac{1}{C_1} + \frac{1}{C_2} + \frac{1}{SC_{\text{m}}}$, and $\tau_{\text{m}} := \frac{SC_{\text{m}}}{g_{\text{e}}}$. The ionic current I_{ion}, state variables h and evolution function g are given by the Beeler-Reuter model. The voltage measured in experiments is now $V = V_1 + V_2 + (R_{\text{w1}} + R_{\text{w2}})I + V_{\text{m}}$. In addition to the parameters S and g_{e}, we need to determine the parameters R_1, τ_1 and R_2, τ_2 that characterize each electrode.

3 Calibration from Bench Experiments

In order to evaluate the accuracy of the parallel R-C model for the electrode polarization, we measure the current I and the voltage V delivered by pacemaker leads directly in a saline solution, without cardiac tissue (Fig. 3, left). We used a Microport CRM Borea DR pacemaker, with a Vega lead in a solution with measured conductivity 2.85 mS cm^{-1}, to obtain 9 datasets of current and voltage (I_{meas} and V_{meas}). The datasets differ exclusively by the amplitude (1, 2 or 4 V) and duration (0.25, 0.5 or 1 ms) of the delivered pulse.

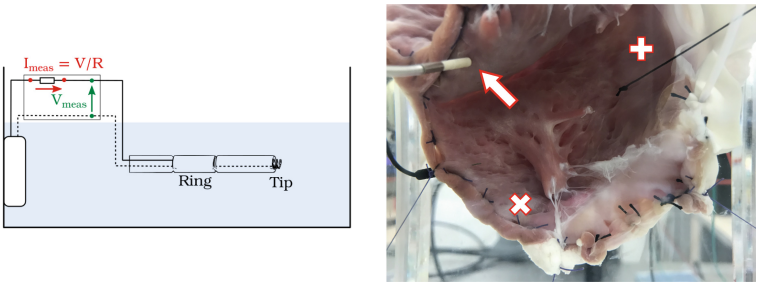

Fig. 3. Left: sketch of the bench test used to calibrate the electrode contact model. Right: right ventricle endocardial view of the tissue wedge preparation with the pacemaker electrode implanted in the septum (pointed by arrow). Other implantations sites were located in the apex (×) and at the base of the ventricle (+).

The experimental setup can be modelled by the circuit shown in Figs. 1 (left and middle), where we used the equivalent circuit from the previous section for the pacemaker, and R_{bath} denotes the resistance of the saline medium. The corresponding differential equations system (1) has 5 parameters to be identified: R_{bath} and the properties of the contacts R_1, R_2, τ_1 and τ_2. The parameter R_{bath} was deduced from the measured initial conditions, as the electrodes are considered depolarized: $R_{\text{bath}} = \frac{V_{\text{meas}}(t=0)}{I_{\text{meas}}(t=0)} - R_{\text{w2}} - R_{\text{w1}}$. The four remaining parameters $\theta = (R_1, R_2, \tau_1, \tau_2)$ were calibrated using the following cost function:

$$J(\theta) = \sum_{\text{s}} \omega_{\text{s}} \mathbb{1}_{\text{s}}(t) \left(\frac{\|V(\theta) - V_{\text{meas}}\|_{\ell^2}}{\|V_{\text{meas}}\|_{\ell^2}} + \frac{\|I(\theta) - I_{\text{meas}}\|_{\ell^2}}{\|I_{\text{meas}}\|_{\ell^2}} \right),$$

where ω is a vector of three weights of sum 1 that allows to give more importance on a specific step, $\text{s} \in \{\text{pulse, switch, OCD}\}$. The function $\mathbb{1}_{\text{s}}$ restricts the computation of the relative difference of the ℓ^2 norms of voltage and current on a specific step, V_{meas} and I_{meas} are the experimental data of the voltage and current, and $V(\theta)$ and $I(\theta)$ are the numerical solutions of the voltage and current, respectively. We used the SciPy implementation of the L-BFGS-B algorithm to minimize the cost function J within a subset of $\mathbb{R}^4$ for θ. Each evaluation of J requires to solve system (1) that is linear in I, V_1 and V_2. We

solve it semi-analytically using eigenvalue decomposition at each time step in a dedicated Python code. The convexity of J was not established. Hence, we first optimize the logarithm of each parameter ($R \in [1, 10^5]$ Ω for the resistances, and $\tau \in [10^{-6}, 1]$ s for the characteristic times), in order to fix a correct order of magnitude, and then fit the values of the parameters.

First, the model was calibrated using the 9 data files separately. For each file, and for a given choice of Ω, the L-BFGS-B algorithm was started at a value of the parameters θ for which the cost function $J(\theta)$ is the lowest among 10 000 random samples of θ. Then, we minimized J using the 9 files all at once, with the average value of the previously found parameters as starting point. We set $\omega = (0.45, 0.45, 0.1)$, so as to emphasize the steps in which the information can be more easily recovered.

The results of the fits are illustrated on Fig. 4, for both voltage and current. We found that one of the couples of parameters is well determined: $R_2 = 26.0 \pm 1.77$ Ω, $\tau_2 = 0.0548 \pm 6.93\ 10^{-3}$ ms ($C_2 = 2.12 \pm 0.34$ µF). However, we found values of R_1 with much larger variability across the files: between 2 and 6 kΩ, with average $\sim$ 4 kΩ, which is one order of magnitude larger than the total impedance measured by the device (940 Ω). We believe that it is due to the over-simplification of our contact model, leading to this equivalent resistance having no real physical meaning. We tried to use more complex models to reproduce the data during the OCD step, to overcome this limitation of the simple R-C parallel model. However, we faced problems of identifiability of the parameters during the calibration (*ie*, finding different local minima for repeated computations).

Anyway, the currents produced by the parallel R-C model are close to the data, and consequently, we consider this model to be accurate enough as a current source for the cardiac model.

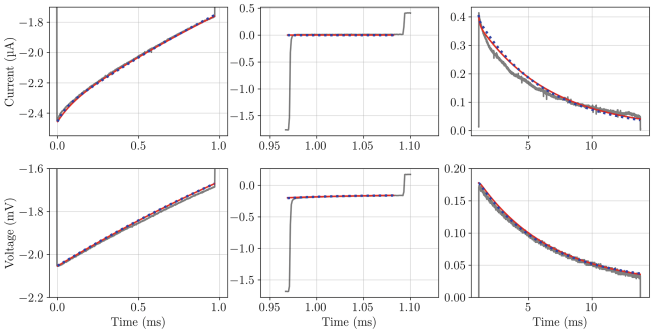

Fig. 4. Fitted currents and voltages when calibrating parameters $\theta = (R_1, R_2, \tau_1, \tau_2)$. Gray solid lines are one experimental dataset, blue dotted lines are computed with θ calibrated with this dataset, and red solid lines from the calibration of the 9 datasets together. (Color figure online)

4 Numerical Results, Comparison with Animal Experiments

Simulation of Single Stimulations, Computation of Lapicque Curves. With all parameters set, we computed the solutions of Eqs. (2) using the same software. An example of simulated transmembrane voltage is given on Fig. 5 (left), for 5 stimulations of 428.5 mV and 1 ms, with $S = 50$ cm^2 and $g_e = 0.01$ mS at 90 bpm. This set of parameters results in several captures and non-captures, due to variables of the Beeler-Reuter model that do not return to their original state between each pulse. This shows that a single stimulation with these parameters is not sufficient to trigger a complete depolarization.

From transmembrane voltages, we extract the ratio of successful captures (60% in the illustrated case). We can compute this ratio for several amplitudes V_{stim} and durations d of stimulation, following a 2D dichotomy algorithm in the Lapicque space (Fig. 5 right). The algorithm detects when the capture ratio exceeds 50%, and returns a collection of intervals that should contain the Lapicque curve. We then compute the rheobase V_{rh} (V) and chronaxie T_{ch} (S) of Lapcique's law $V_{\text{stim}}(d) = V_{\text{rh}}(1 + T_{\text{ch}}/d)$ that best match the midpoints of these intervals. Our model seems in agreement with this law, for the set of parameters used to generate Fig. 5.

We then computed several Lapicque curves, for other values of S and g_e, and compared the results with experimental data described in the next paragraph.

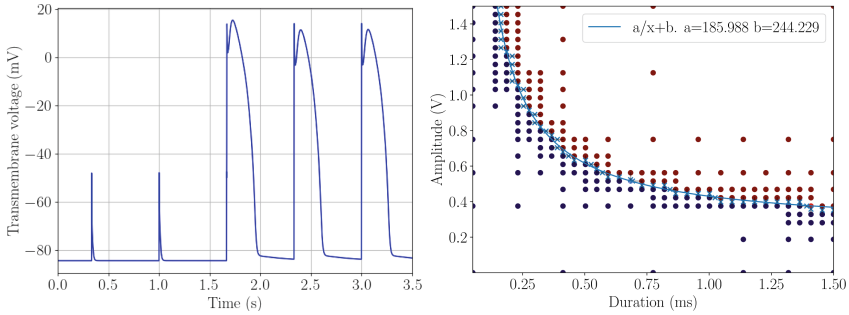

Fig. 5. Transmembrane voltage (left) computed for a single set of parameters $(V_{\text{stim}}, d, S, g_e)$; and Lapicque curve (right) obtained after detection of a 50% capture ratio. Blue points are for 0% capture, and red points for 100% capture. (Color figure online)

Ex-vivo Measurements. Isolated coronary-perfused ventricular wedge preparations were carried out on two sheep hearts, as described in [5]. Perfusion leaks along cut surfaces were carefully occluded for homogeneous perfusion resistance across the preparation. The wedge preparation was then stretched on to a frame to immobilize the tissue into a bath of saline solution (Fig. 3, right).

To study the MicroPort lead (contacts characteristics and voltages applied to the tissue), three lead implantation regions were identified (RV apex, RV

septum and RV basal sites) and the lead was implanted in the heart by fully deploying the screw electrode perpendicularly to the tissue's surface. Electrocardiography (ECG) and electrograms (EGM) measured with the lead were simultaneously recorded through an independent acquisition system (PowerLab, ADInstruments). The EGMs were also measured with the pacemaker.

We tested a range of pulse durations and stimulus amplitudes to localize the stimulation threshold. Due to the limited number of steps in stimulation amplitude and duration of the pacemaker, the measured data points cover only sparsely the Lapicque plane. Nevertheless, these data can later be used for fitting the computational model responses to lead stimuli.

Comparison Between Experiment and Simulation. From experimental data, we identified, for each pacing pulse duration, the minimum pulse amplitude that captured. Below this pulse amplitude, any stimulation fails to capture the tissue. We could therefore define a region, delimited on the top by the lowest capturing amplitude, and on the bottom by the highest non-capturing amplitude, in which the Lapicque curve should be found (Fig. 6).

We show from the 0D model that the parameter S has great influence, since it determines the amount of current seen by square centimeter of membrane. On the contrary, we found very little influence of the parameter g_e on the output (not shown). We also studied the influence of parameters of the bio-electrode contact, by varying the resistance R_1. This is justified by the fact that the tip electrode is not any more in contact with a saline solution only, but with the cardiac tissue too (Fig. 6 right).

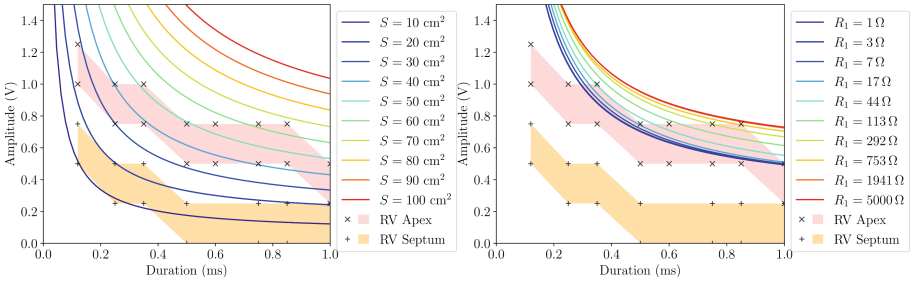

Fig. 6. Comparison of Lapicque curves (solid lines) computed with different values of S (left) and R_1 (right). The shaded regions indicate where the experimental capture threshold is located, for different stimulation sites on the tissue wedge.

The fits of Lapicque law $V_{\text{stim}} = V_{\text{rh}}(1 + T_{\text{ch}}/d)$ do not fall within these regions for all durations. This is expected because the parameters S ad g_e of the 0D model cannot be completely characterized, as surrogates of the geometry and electric conductivity coefficients of the real tissue. Additionally, these parameters may depend on the amplitude of the stimulation, as the excited volume of tissue may change. As a consequence, further calibration work is required, especially to determine the parameter S which plays a crucial role in this 0D model.

5 Conclusion

In this paper, an innovative model is proposed, which couples a pacemaker electrical circuit to equations modeling cardiac action potential, accounting for the complex physics at the bio-electrode interfaces. Animal experiments were conducted which provide information on the electrical function of a cardiac tissue sample stimulated by a commercial pacemaker. It allows us to compare Lapicque curves obtained with the numerical model with experimental capture data.

It is noticeable that the literature provides no model for coupling a pacemaker to a cardiac tissue, because all studies focus either on characterizing in-depth the physics of the bio-electrode contact, or on characterizing the onset of cardiac activation in the tissue sample (virtual electrodes, make and break activations, etc.). To our knowledge, this work provides a first possible model that links the energy delivered by the pacemaker to the onset of activation, trying to evaluate with a model the real distribution of energy between all the concerned elements, pacemaker circuit, bio-electrical contact, and cardiac tissue. The model proposed in this article includes many simplifications, for example it assumes that the contact properties calibrated from bench experiments do not change when the contact is made with cardiac tissue. However, we prefered not to use a more descriptive model that could not be validated against the experimental data at hand.

We are currently deriving and implementing a more reliable 3D model, with bidomain equations for the cardiac tissue in blood. This model will characterize more accurately the delivery of current into cardiac cells, accounting for the spatial distribution of current. In any case, in order to derive such a 3D model and computational solver, we need to calibrate the bio-physical parameters with respect to experimental conditions. The calibration and validation process will benefit from data that were recorded, alongside the EGMs described in the previous section. In addition, optical mapping data were also recorded. They may allow us to better monitor the propagation of the action potential in the tissue. High resolution 9.4T MR images of the anatomy were also acquire, so as to better characterize the tissue structure, prior to simulations.

We also plan to use better techniques than a 2D dichotomy to localize the simulated Lapicque curves, which will reduce the computational burden that will arise when using 3D bidomain equations.

Acknowledgements. This work was supported by the H2020 EU SimCardioTest project (Digital transformation in Health and Care SC1-DTH-06-2020; grant agreement number 101016496). This study received financial support from the French Government as part of the "Investments of the Future" program managed by the National Research Agency (ANR), Grant reference ANR-10-IAHU-04. Experiments presented in this paper were partially carried out using the PlaFRIM experimental testbed, supported by Inria, CNRS (LABRI and IMB), Université de Bordeaux, Bordeaux INP and Conseil Régional d'Aquitaine.

References

1. Beeler, G.W., Reuter, H.: Reconstruction of the action potential of ventricular myocardial fibres. J. Physiol. **268**(1), 177–210 (1977)
2. Blair, H.: On the intensity-time relations for stimulation by electric currents. I. J. Gen. Physiol. **15**(6), 709–729 (1932)
3. Grimnes, S., Martinsen, O.G.: Bioimpedance and Bioelectricity Basics, 3rd edn. Academic Press, Oxford (2015)
4. Somersalo, E., Cheney, M., Isaacson, D.: Existence and uniqueness for electrode models for electric current computed tomography. SIAM J. Appl. Math. **52**(4), 1023–1040 (1992)
5. Walton, R.D., et al.: Compartmentalized structure of the moderator band provides a unique substrate for macroreentrant ventricular tachycardia. Circ.: Arrhythmia Electrophysiol. **11**(8), e005913 (2018)